Electronic Supplementary Material (ESI) for Polymer Chemistry.
This journal is © The Royal Society of Chemistry 2022

Supplementary Information for

Influence of the molecular weight and size distribution of PSS on mixed ionic-electronic transport in PEDOT:PSS

Chun-Yuan Lo,[1] Yuhang Wu,[2] Elorm Awuyah,[1] Dilara Meli,[3] Dan My Nguyen,[1] Ruiheng Wu,[4] Bohan Xu,[3] Joseph Strzalka,[5] Jonathan Rivnay,[6,7] David C. Martin,[2,8] and Laure V. Kayser*[1,2]

[1]*Department of Chemistry and Biochemistry, University of Delaware, Newark, Delaware, 19716*
[2]*Department of Materials Science and Engineering, University of Delaware, Newark, Delaware, 19716*
[3]*Department of Materials Science and Engineering, Northwestern University, Evanston, Illinois 60208*
[4]*Department of Chemistry, Northwestern University, Evanston, Illinois 60208*
[5]*X-Ray Science Division, Argonne National Laboratory, Lemont, Illinois 60611*
[6]*Department of Biomedical Engineering, Northwestern University, Evanston, Illinois 60208*
[7]*Simpson Querrey Institute, Northwestern University, Chicago, Illinois 60611*
[8] *Department of Biomedical Engineering, University of Delaware, Newark, Delaware, 19716*

*Author to whom correspondence should be addressed: lkayser@udel.edu

GENERAL

Materials

Sodium 4-styrenesulfonate (NaSS), 4,4′-azobis(4-cyanovaleric acid) (ACVA), 3,4-ethylenedioxythiophene (EDOT), sodium persulfate ($Na_2S_2O_8$), iron(III) sulfate ($Fe_2(SO_4)_3$), ethylene glycol (EG), dodecylbenzenesulfonic acid (DBSA), (3-glycidyloxypropyl) trimethoxysilane (GOPS), acidic resin (Dowex Marathon C hydrogen form), base resin (Lewatit MP-62 free base), and the RAFT chain transfer agent 4-cyano-4-(phenylcarbonothioylthio) pentanoic acid (**CTA 1**) and 2-cyanopropan-2-yl N-methyl-N-(pyridin-4-yl)carbamodithioate (**CTA 2**) were purchased from Sigma-Aldrich and used without further purification. Distilled water filtered using a Milli-Q purification system was used throughout. Screen-printed electrodes (SPE), catalog NO. C233BT purchased from Metrohm, consists of a round gold working electrode at a diameter of 1.6 mm, surrounded by a gold counter electrode and a silver pseudoreference electrode (-0.133 V vs. Ag/AgCl). The connection tracks are made of silver. Interdigitated electrodes (IDE), catalog NO. G-IDEAU5 was also purchased from Metrohm, unlike those SPEs, only two 5-µm-wide interdigitated gold electrodes with two gold connection tracks are deposited.

Synthesis of PSS with a narrow molecular weight dispersity.

NaSS (1.83 g, 8.86 mmol), 4-Cyano-4-(phenylcarbonothioylthio)pentanoic acid (**CTA 1**) (14 mg, 0.05 mmol). ACVA (2.8 mg, 0.01 mmol) were added to a 50 mL two-neck round bottom flask at room temperature and dissolved in 6 mL water and 2 ml ethanol, then degassed with nitrogen for 30 mins. The reaction mixture was placed in an oil bath at 70 °C and left to react for 24 hours. The reaction was stopped by rapid cooling and exposure to air. PSSNa was purified by precipitation in acetone and dried under vacuum. PSSNa was dissolved in water (0.5 g mL^{-1}) and stirred over an acidic resin (Dowex Marathon C hydrogen form) for 6 h at room temperature to afford poly(styrene sulfonic acid) (PSS). Then, PSS was filtered through a 0.45 µm Nylon syringe filter and dried under vacuum.

Synthesis of PSS with a broad molecular weight dispersity.

The broad range of PDI of PSSNa samples was obtained by using 2-cyanopropan-2-yl N-methyl-N-(pyridin-4-yl)carbamodithioate (**CTA 2**) as RAFT agent. The procedure was same as the one used for the synthesis of PSS with a narrow molecular weight dispersity. Then, PSSNa was dissolved in water (0.5 g mL^{-1}) and stirred over an acidic resin for 6 hours at room temperature to afford poly(styrene sulfonic acid) (PSS). Then, PSS was filtered through a 0.45 µm Nylon syringe filter and dried under vacuum.

Synthesis of PSS with a broad molecular weight dispersity by using the combination of chain-transfer agents.

The broad range of PDI of **PSS 32k-1.7** sample was obtained by choosing mixtures constituting of 50% **CTA 1** and 50% **CTA 2** as RAFT agent. The procedure was same as the one used for the synthesis of PSS with a narrow molecular weight dispersity.

General procedure for the synthesis of PEDOT:PSS. PSS (0.14 g, 0.82 wt %) was dissolved in 15 g of DI water and stirred until fully dissolved. Then, sodium persulfate (130 mg, 1.2 mmol) and 10 wt % iron sulfate solution (30 µl, 0.2 mmol) were added and stirred vigorously for 10 mins before the addition of EDOT (42 µl, 1.07 mmol), additionally, added 2 ml of DI water after stirring 4 hours. The reaction was stirred at 13 °C for 20 hours. Then, PEDOT:PSS was purified over 3.6 mL of acidic (Dowex Marathon C hydrogen form) and 2 mL of basic (Lewatit MP-62 free base) resins for 6 h at room temperature and then filtered through a 10 µm filter.

OECT fabrication. OECT configuration see Figure S1. In order to evaluate the capacitive behaviors and impedance amplitudes of materials studied in this work as well as the characteristics of OECTs fabricated from them, one IDE and one SPE were paired together as Figure S1. For OECTs, this configuration is usually referred to as the side-gated configuration and was also adopted in other works.[1–3] To achieve this configuration, the preparation of the PEDOT:PSS films, 3.8 mL of PEDOT:PSS aqueous dispersion were mixed with 5 volume% ethylene glycol (EG, 200 µL), 0.1 volume% dodecyl benzene sulfonic acid (DBSA, 4 µL), and 1 volume% of (3-glycidyloxypropyl) trimethoxysilane (GOPS, 40 µL). The resulting PEDOT:PSS suspension solution was first spin-coated at 800 rpm for 60s then 2000 rpm for 60s on the ozone-cleaned IDE. The film thicknesses were measured using a Bruker, Dektak XT surface profilometer.

Also, the thickness of the spin-casted film was intentionally controlled by putting different numbers of layers on the substrate.[4] This was performed by repetitively spin-coating and a quick bake at 100 ˚C for five minutes between each spin-coating step. Then the Kapton tape was used to define the area directly exposed to the aqueous electrolyte (0.1 M KCl) in the gold connection track area (as shown in Figure S1) with a well-defined length of 1.7 mm (L_c). The application of the Kapton tape in this work is not only for insulating the part other than the active channel but also for creating different aspect ratios of channel areas for the following studies on the scaling behaviors of the peak transconductance (g_m). After that, an SPE was placed parallelly to the IDE ensuring the reference electrode was in the vicinity of the channel. Enough electrolyte was transferred on the PEDOT:PSS covered gold connection track on IDE as well as gate (original reference) electrode and the auxiliary electrode (original working) on SPE for performing subsequent characterizations. Because of the hydrophilicity of PEDOT:PSS and the hydrophobicity of the Kapton tape, the channel area was well-covered in all devices.

Characterization

^{1}H NMR spectra were obtained by using Bruker 400 MHz spectrometers. Sample solutions of the polymer were prepared in D_2O. Number-average (M_n) and weight-average (M_w) molecular weights and dispersity were determined by HLC-8420 GPC EcoSEC LC system running in 20 % methanol and 70 % 0.3 M $NaNO_3$, 0.01 M NaH_2PO_4 in water at 25 °C (0.8 mL min^{-1}), using two PL aquagel-OH Mixed-H (8μm 50*7.5) columns, and calibrated against narrow dispersity polystyrene sulfonate standards (purchased from Polymer Standards Service). The elemental composition of the PEDOT:PSS film surface was analyzed by X-ray photoelectron spectroscopy (Thermo Fischer Scientific, K-Alpha XPS, Avantage). The samples for atomic force microscopy (AFM) thin films were prepared by spin-coating at 800 rpm for 60s then 2000 rpm for 60s on quartz substrates. The AFM images were acquired in a tapping mode (Bruker, The MultiMode AFM, NanoScope analysis) in a 500 nm × 500 nm scanning area at a rate of 1 Hz. Preparation of samples for conductivity measurements, glass slides were cut into 2.54 cm squares with a diamond-tipped scribe. The slides were then successively washed in Alconox solution (2 mg mL^{-1}), deionized water, acetone, and isopropyl alcohol (IPA) in an ultrasonic bath for 10 min each and dried with compressed air. The glass slides were then plasma treated at ~30 W for 60 s at a pressure of 200 mTorr under ambient air to remove any residual organic material and activate the surface. The PEDOT solutions were spin-coated onto glass slides at a spin speed of 500 rpm (250 rpm s^{-1} ramp) for 120 s followed by 2000 rpm (1000 rpm s^{-1} ramp) for 30 s. After spin-coating the samples were annealed on a hotplate at 120 °C for 15 mins under a nitrogen flow. And the resistance was measured by using the Ossila Four-Point Probe System and Keithley 2400 source meter. The thickness of the films was measured using a J.A. Woolam M-2000VI Ellipsometer to convert the resistance to conductivity. The conductivity σ was calculated inverse value of sheet resistance times sheet thickness and an average conductivity of 3 independently synthesized PEDOT:PSS samples.

Cyclic voltammetry (CV) and electrochemical impedance spectroscopy (EIS) were carried out on a Solartron Analytical Modulab potentiostat/galvanostat, in which the source and drain were connected to the working and working sense electrodes together. The silver pseudoreference of SPE was used as the reference electrode and the working electrode was used as the auxiliary electrode. 0.1 M KCl aqueous solution was used throughout all characterizations done in this work. CV was repeated from 0 to 0.5 V at 0.1 V s^{-1} until the stable cycle was achieved. EIS was recorded from 10^{-1} to 10^{-5} Hz with an amplitude of 10 mV at the background voltage of 0 V.

The OECTs fabricated and assembled as Figure S1 were evaluated on a Keithley 2612B dual-source measurement unit. The silver pseudoreference on an SPE was used as the gate electrode and the working electrode was disconnected under this scenario. Two gold connection tracks on IDE were designated as the source and drain electrodes as Figure S1. The output curves of each

OECT were collected when the drain voltage (V_D) swept from 0 to -0.6 V at the increment of -0.01 V with the varied gate voltage (V_G) from -1.0 to 1.0 V at the increment of 0.1 V. The transfer curve of each sample was constructed at V_D = -0.6 V along with V_G varying the same as the output curves. The threshold voltage (V_{Th}) of each OECT was extracted subsequently from the linear regions of their transfer curves.[5, 6] The first derivative of each data point was the transconductance (g_m) that was plotted against V_G as well. The peak g_m of each OECT with the channel materials synthesized at different channel dimensions were plotted against the product of channel width (W) and thickness (d) over the channel length (L_c), and the difference between V_{Th} and V_G, i.e., $WdL_c^{-1}(V_{Th} - V_G)$ (Figure S1). The linear fitting with the y-axis intercept at zero offsets was implemented on all three formulas for demonstrating the impact of molecular weights and PDI on the transconductance scaling behaviors of them, as this is one of the important figure-of-merit of OECTs.

Grazing-incidence wide-angle x-ray scattering (GIWAXS) was performed with a photon energy of 10.9 keV at a scattering angle of θ = 0.14 degrees in a helium environment. The experiments were carried out in sector 8-ID-E of the Advanced Photon Source at Argonne National Labs. Data reduction was performed using GIXSGUI and peaks were fit using MATLAB.[7]

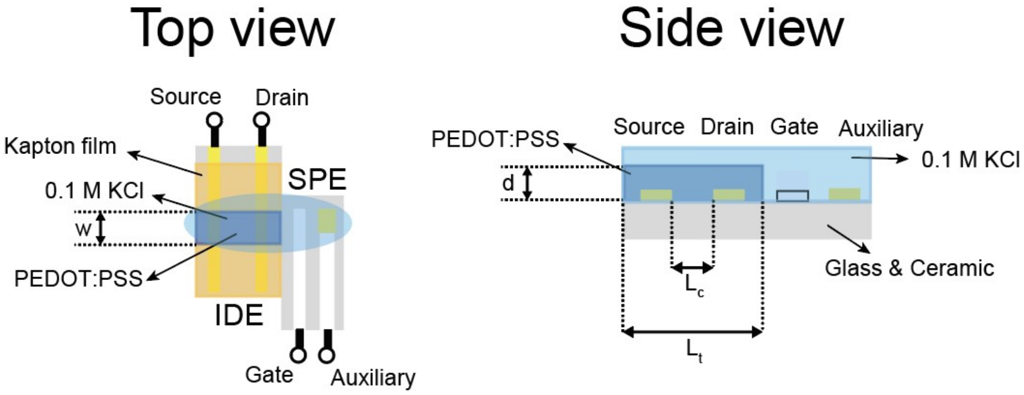

Figure S1. Schematic representation of the OECT devices structure.

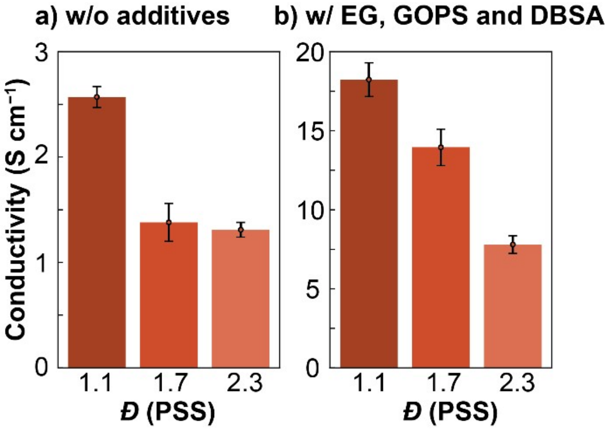

Figure S2. Electrical conductivity of PEDOT:PSS with a molecular weight of approximately 35k with *Đ* = 1.1 and 1.7 (monomodal distributions), and 2.3 (bimodal distribution) as measured by four point probe. **(a)** Without additives. **(b)** With 5 vol% EG, 1 vol% GOPS, and 0.1 vol% DBSA additives.

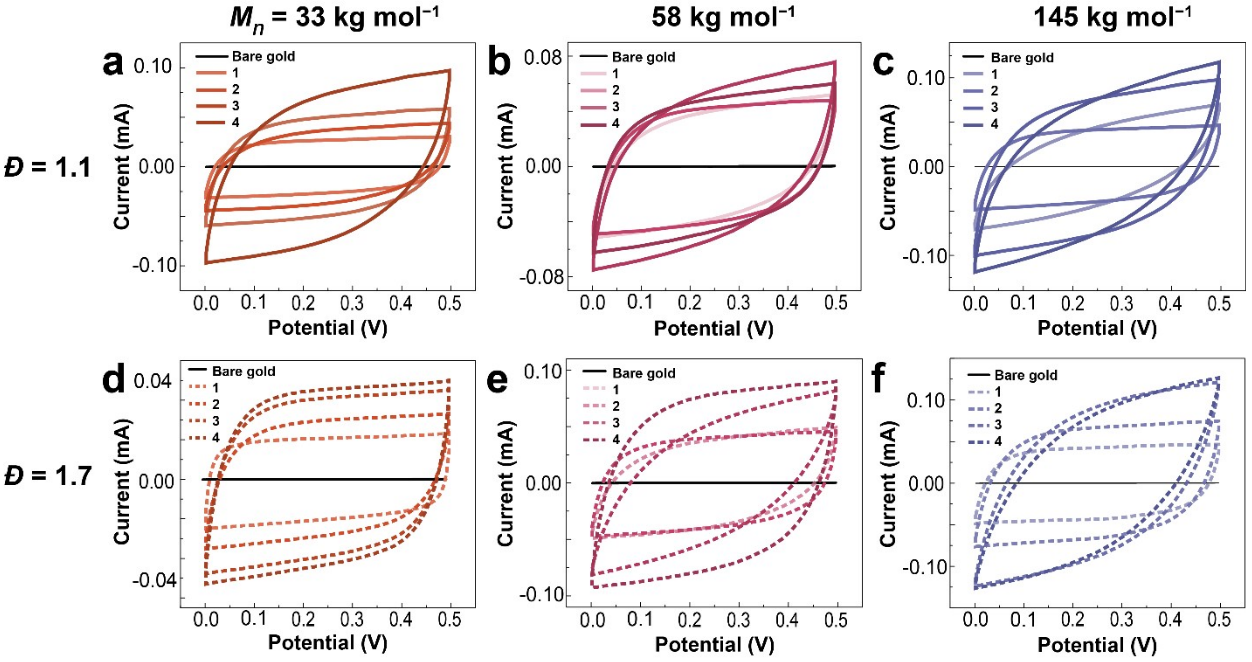

Figure S3. CV scans PEDOT:PSS samples with 5 vol% EG, 1 vol% GOPS, and 0.1 vol% DBSA at different volumes on IDE. **(a)** PEDOT:PSS 33k-1.1, **(b)** PEDOT:PSS 58k-1.1, **(c)** PEDOT:PSS 145k-1.1, **(d)** PEDOT:PSS 32k-1.7, **(e)** PEDOT:PSS 58k-1.7, and **(f)** PEDOT:PSS 144k-1.7.

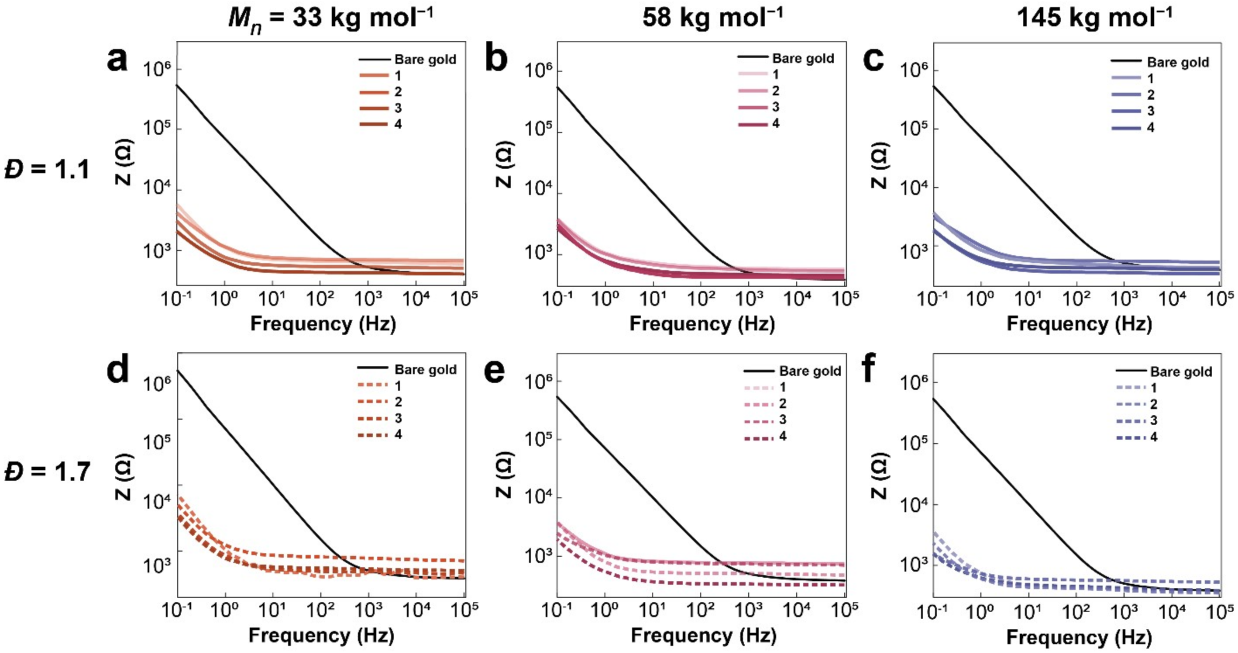

Figure S4. Impedance amplitude of PEDOT:PSS samples with 5 vol% EG, 1 vol% GOPS, and 0.1 vol% DBSA at different volumes on IDE. **(a)** PEDOT:PSS 33k-1.1, **(b)** PEDOT:PSS 58k-1.1, **(c)** PEDOT:PSS 145k-1.1, **(d)** PEDOT:PSS 32k-1.7, **(e)** PEDOT:PSS 58k-1.7, and **(f)** PEDOT:PSS 144k-1.7.

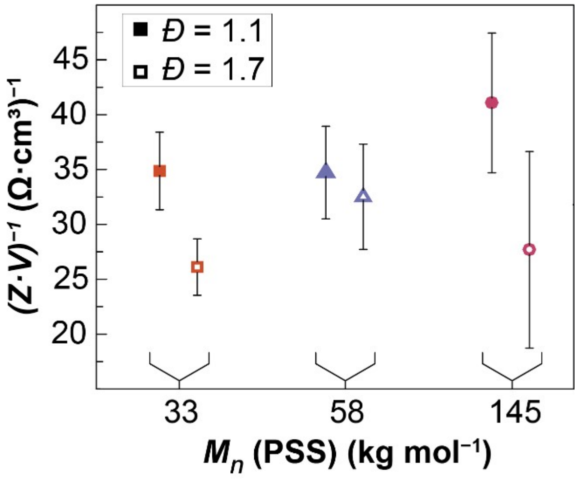

Figure S5. Reciprocal of the average specific impedance at 0.1 Hz for each PEDOT:PSS sample.

Table S1. List of all relevant parameters obtained via EIS fitting to the circuit model (Figure 4 inset).

PEDOT:PSS Sample Name	R_s **(Ω)**	R_c **(Ω)**	C_d **(F)**	Z_o*			**χ²**	**Volume (cm³)**
				R (Ω)	**T (s)**	**P**		
33k-1.1	572.4	28.2	2.8E-7	207.4	0.04	0.4	0.003	1.3E-5
32k-1.7	510.5	18.2	2.3E-6	133.3	0.04	0.4	0.003	1.2E-5
58k-1.1	410.0	1.0	3.7E-6	120.1	0.03	0.4	0.01	1.1E-5
58k-1.7	752.6	8.5	1.6E-6	99.4	0.02	0.4	0.001	1.8E-5
145k-1.1	330.7	6.7	6.1E-6	59.7	0.02	0.4	0.003	1.1E-5
144k-1.7	358.1	33.69	2.6E-6	171.3	0.09	0.4	0.005	2.0E-5

*$Z_o = \frac{R}{(jT\omega)} \cdot cothcoth\,(jT\omega)^p$

Table S2. Dimensions and figures of merit for the OECT devices and measurements.

Sample Name	WdL_c^{-1} **(nm)**	g_m **(mS)**	$(V_{Th} - V_G)$ **(V)**	$[\mu_{OECT}C^*]$ **(F cm^{-1} V^{-1} s^{-1})**	μ_{OECT}**^{a}** **(cm^2 V^{-1} s^{-1})**
PEDOT:PSS 33k-1.1	730	1.4	0.4	31.7 ± 13.9	1.17
	1926	3	0.48		0.79
	986	8.22E-01	0.68		0.30
	1645	3.6	0.51		1.05
	1407	2	0.49		0.71
PEDOT:PSS 145k-1.1	2468	2.8	0.37	32.2 ± 6.8	0.64
	706	1.3	0.64		0.60
	1218	2.2	0.41		0.92
	1450	2.1	0.53		0.57
	1477	2.41	0.45		0.76
PEDOT:PSS 144k-1.7	1970	10.7	0.46	142.4 ± 27.3	3.37
	1266	7	0.51		3.10
	1257	7.14	0.43		3.77
	2610	15.2	0.37		4.50
	2284	16.1	0.39		5.16
	1357	7.31	0.44		3.50

[a] Calculated by dividing $[\mu_{OECT}C^*]$ by the average C^* obtained by CV.

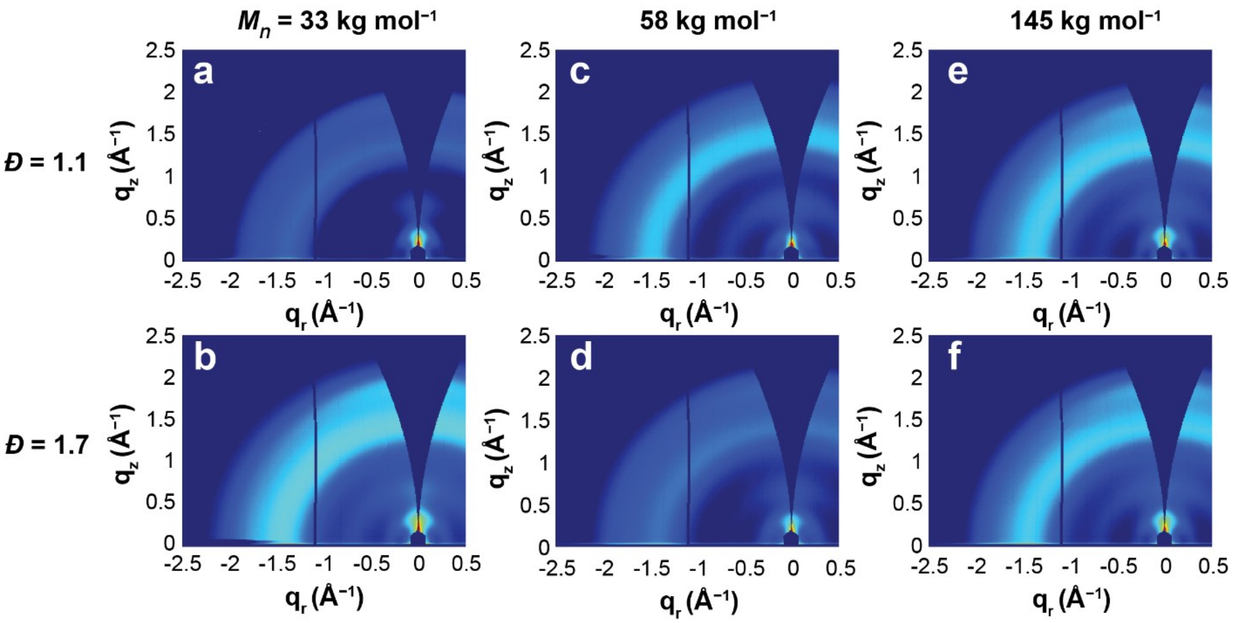

Figure S6. 2-D GIWAXS scattering patterns of the PEDOT:PSS samples with 5 vol% EG, 1 vol% GOPS, and 0.1 vol% DBSA, showing preferential out-of-plane lamellar and isotropic PSS scattering. **(a)** PEDOT:PSS 33k-1.1, **(b)** PEDOT:PSS-32k-1.7, **(c)** PEDOT:PSS 58k-1.1, **(d)** PEDOT:PSS 58k-1.7, **(e)** PEDOT:PSS 145k-1.1, and **(f)** PEDOT:PSS 144k-1.7.

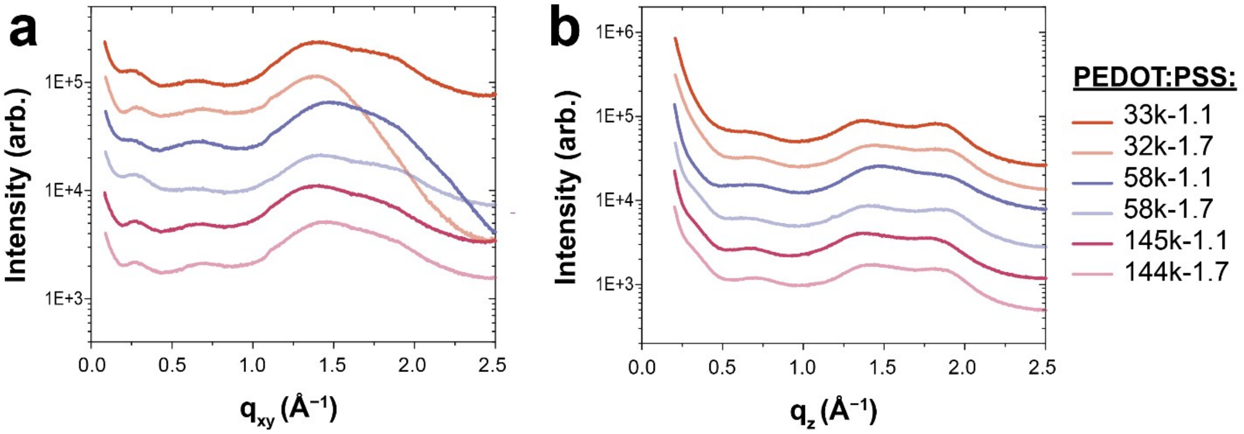

Figure S7. (a) In-plane (q_{xy}) and **(b)** out-of-plane (q_z) linecuts extracted from 2-D GIWAXS scattering patterns of PEDOT:PSS with 5 vol% EG, 1 vol% GOPS, and 0.1 vol% DBSA. PEDOT:PSS- 32k-1.7 and -58k-1.1 show rapidly decreasing scattering intensity at q > 1.5 Å^{-1} due to a shadowing artifact.

Table S3. In-plane and out-of-plane peak distances (d) and coherence lengths (Lc) extracted from peak fitting

	In-plane				**Out-of-plane**	
PEDOT:PSS	**d_{100} (Å)**	**Lc_{100} (Å)**	**$d_{1'00}$ (Å)**	**$Lc_{1'00}$ (Å)**	**d_{π} (Å)**	**Lc_{π} (Å)**
33k-1.1	23.8	31.9	10.0	12.5	3.40	13.9
32k-1.7	21. 5	35.2	9.55	9.87	3.34	16.6
58k1.1	26.6	22.4	9.70	10.5	3.34	13.7
58k-1.7	22.3	38.4	9.66	-	3.34	15.4
145k-1.1	22.2	27.8	9.68	12.9	3.47	15.5

144k-1.7	22.0	22.8	9.22	15.5	3.38	15.6

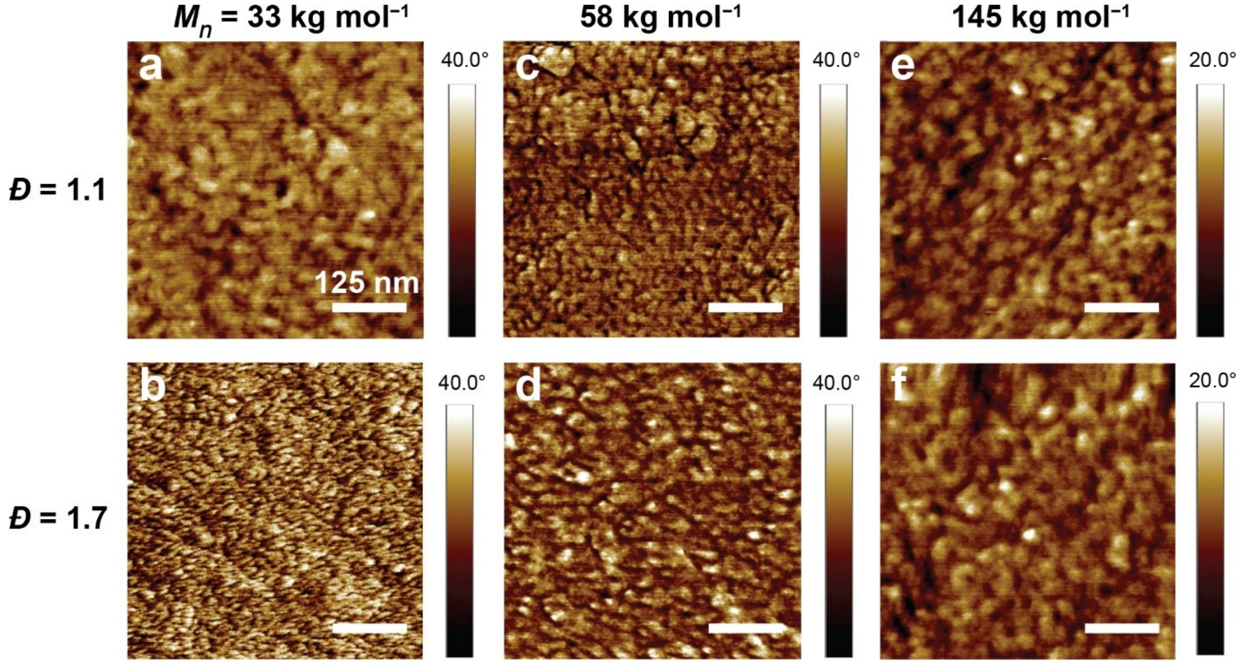

Figure S8. AFM phase images of PEDOT:PSS thin films without additives. (a) PEDOT:PSS 33k-1.1, **(b)** PEDOT:PSS-32k-1.7, **(c)** PEDOT:PSS 58k-1.1, **(d)** PEDOT:PSS 58k-1.7, **(e)** PEDOT:PSS 145k-1.1, and **(f)** PEDOT:PSS 144k-1.7. Scale bar: 125 nm.

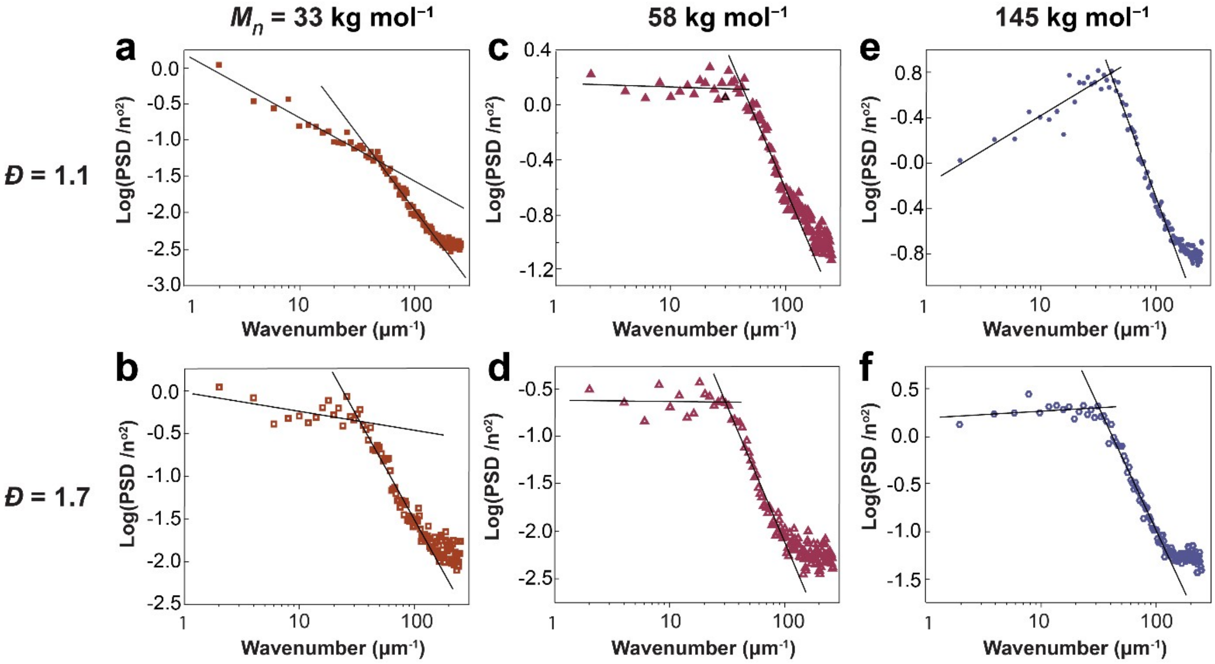

Figure S9. PSD analysis. log(PSD)–log(f) for the AFM phase images shown in Figure 7 showing two wavelength regimes that satisfy the power law relationships. **(a)** PEDOT:PSS 33k-1.1, **(b)** PEDOT:PSS 58k-1.1, **(c)** PEDOT:PSS 145k-1.1, **(d)** PEDOT:PSS 32k-1.7, **(e)** PEDOT:PSS 58k-1.7, and **(f)** PEDOT:PSS 144k-1.7.

Table S4. Domain dimensions extracted from the PSD analysis of the AFM phase images of all the PEDOT:PSS films.

PEDOT:PSS Sample Name	Wavenumber at cross-section (μm^{-1})	Domain size (nm)	Slope of the fitting line from the high frequency region	R^2
33k-1.1	46	22	-2.14±0.05	0.97
32k-1.7	33	30	-2.42±0.07	0.96
58k-1.1	42	24	-1.95±0.07	0.95
58k-1.7	28	36	-2.89±0.09	0.96
145k-1.1	42	24	-2.77±0.05	0.98
144k-1.7	32	31	-2.61±0.05	0.98

REFERENCES

1 Koutsouras, D. A., F. Torricelli, P. Gkoupidenis, P. W. M. Blom. Efficient Gating of Organic Electrochemical Transistors with In-Plane Gate Electrodes. *Adv. Mater. Technol.*, **2021**, 2100732.

2 Koutsouras, D. A., K. Lieberth, F. Torricelli, P. Gkoupidenis, P. W. M. Blom. Selective Ion Detection with Integrated Organic Electrochemical Transistors. *Adv. Mater. Technol.*, **2021**, 2100591.

3 Wei, Q., M. Mukaida, Y. Naitoh, T. Ishida. Morphological Change and Mobility Enhancement in PEDOT:PSS by Adding Co-Solvents. *Adv. Mater.*, **2013**, *25*, 2831.

4 Bianchi, M., S. Carli, M. Di Lauro, M. Prato, M. Murgia, L. Fadiga, F. Biscarini. Scaling of Capacitance of PEDOT:PSS: Volume vs. Area. *J. Mater. Chem. C*, **2020**, *8*, 11252.

5 Friedlein, J. T., R. R. McLeod, J. Rivnay. Device Physics of Organic Electrochemical Transistors. *Org. Electron.*, **2018**, *63*, 398.

6 Bittle, E. G., J. I. Basham, T. N. Jackson, O. D. Jurchescu, D. J. Gundlach. Mobility Overestimation Due to Gated Contacts in Organic Field-Effect Transistors. *Nat. Commun.*, **2016**, *7*, 10908.

7 Jiang, Z. GIXSGUI: A MATLAB Toolbox for Grazing-Incidence X-Ray Scattering Data Visualization and Reduction, and Indexing of Buried Three-Dimensional Periodic Nanostructured Films. *J. Appl. Crystallogr.*, **2015**, *48*, 917.